Biochemical Journal (2019) **476** 2111–2125
https://doi.org/10.1042/BCJ20190154

Research Article

Sugar beet hemoglobins: reactions with nitric oxide and nitrite reveal differential roles for nitrogen metabolism

Nélida Leiva Eriksson[1], Brandon J. Reeder[2], Michael T. Wilson[2] and Leif Bülow[1]

[1]Department of Chemistry, Lund University, Box 188, 221 00 Lund, Sweden; [2]School of Biological Sciences, Essex University, Wivenhoe Park, Colchester CO4 3SQ, U.K.

Correspondence: Nélida Leiva Eriksson (nelida_leiva.eriksson@tbiokem.lth.se)

In contrast with human hemoglobin (Hb) in red blood cells, plant Hbs do not transport oxygen, instead research points towards nitrogen metabolism. Using comprehensive and integrated biophysical methods we characterized three sugar beet Hbs: BvHb1.1, BvHb1.2 and BvHb2. Their affinities for oxygen, CO, and hexacoordination were determined. Their role in nitrogen metabolism was studied by assessing their ability to bind NO, to reduce nitrite (NiR, nitrite reductase), and to form nitrate (NOD, NO dioxygenase). Results show that BvHb1.2 has high NOD-like activity, in agreement with the high nitrate levels found in seeds where this protein is expressed. BvHb1.1, on the other side, is equally capable to bind NO as to form nitrate, its main role would be to protect chloroplasts from the deleterious effects of NO. Finally, the ubiquitous, reactive, and versatile BvHb2, able to adopt 'open and closed forms', would be part of metabolic pathways where the balance between oxygen and NO is essential. For all proteins, the NiR activity is relevant only when nitrite is present at high concentrations and both NO and oxygen are absent. The three proteins have distinct intrinsic capabilities to react with NO, oxygen and nitrite; however, it is their concentration which will determine the BvHbs' activity.

Introduction

The current availability of numerous sequenced genomes has extended our knowledge of the diversity of hemoglobins (Hbs) in living organisms. In vertebrates, Hbs were historically recognized as oxygen transporters. However, phylogenetic analyses have demonstrated that all Hbs are likely to have emerged from a bacterial single-domain globin that showed one or more intrinsic enzymatic functions [1]. This globin later evolved in multicellular eukaryotes with new properties, including reversible binding of diatomic ligands, such as oxygen, carbon monoxide (CO), nitric oxide (NO), and hydrogen sulfide which enabled transport and storage, and detoxification functions [2]. In land plants, two different types of Hbs have been identified: symbiotic (sHbs) and non-symbiotic (nsHbs). NsHbs are functionally and genetically distinct from sHbs, they exhibit the classical myoglobin-fold (Mb-fold), and can be divided into class-1, -2, and -3 [3]. All together, plant Hbs have been renamed to phytoglobins [4]. In monocot plants such as rice and barley, only class-1 nsHbs have been found. Eudicot plants such as Arabidopsis, on the other hand, have both class-1 and class-2 nsHbs. Class-3 nsHbs, also known as truncated Hbs (trHbs), have been found in all plants and resemble the truncated globins found in bacteria [3]. Nodulating eudicot plants additionally have sHbs which are known as Leghemoglobins (Lbs) [4,5].

Unlike oxygen-transporting Hbs from vertebrates and legumes, also known as pentacoordinated Hbs because their heme iron is only bound to the protein by a proximal histidine, most nsHbs are hexacoordinated due to a distal histidine that reversibly binds to the sixth coordination site of the heme iron [6–8]. As demonstrated by ligand binding studies, the mechanisms used to establish

Received: 7 March 2019
Revised: 23 June 2019
Accepted: 8 July 2019

Accepted Manuscript online: 8 July 2019
Version of Record published: 31 July 2019

Biochemical Journal (2019) 476 2111–2125
https://doi.org/10.1042/BCJ20190154

appropriate binding kinetics (and thus affinities) and distinct fractions of hexacoordination in different Hbs involve the combined interactions of the proximal and distal histidines, affecting for instance, their oxygen affinity [3,9].

When referring to the physiological role of plant Hbs, it is widely accepted that they are unlikely to act as oxygen transporters mainly due to their low oxygen dissociation constants [3] and often low concentrations in the cell. Instead, it has been suggested that plant Hbs are involved in nitrogen metabolism and the following activities have been proposed: (i) NO dioxygenase (NOD) [10], (ii) nitrite reductase (NiR) [11,12], and (iii) hydroxylamine reductase [13]. It has also been suggested that the activity of plant Hbs may depend on the level of oxygenation [12] or on the presence of a specific substrate [13]. However, a lack of consensus exists and the functions of these proteins remain unclear. What is clear is that regardless of the reactions plant Hbs perform, they are limited by the rates at which they can be reduced to their active ferrous form [14–16].

The knowledge described above about plant nsHbs has been gained mainly from monocot plants [12,13,17] and one eudicot [11], all of them species that diverged later in the evolution. There is a need for data on more divergent species which would allow us to compare the activities of nsHbs more widely and thus evaluate the significance of their roles in each organism [12,18].

Sugar beet (*Beta vulgaris* ssp. *Vulgaris*) is a member of the order Caryophyllales. This group comprises angiosperms that emerged early, just after the divergence of monocot and eudicot plants and it includes several crops of great economic importance to the food and energy industries [19,20]. In a previous study, three nsHbs were found in sugar beet, BvHb1.1, BvHb1.2 (class-1), and BvHb2 (class-2). A holistic study of their expression indicated that both class-1 were highly expressed during germination while BvHb2 was mainly expressed during the vegetative stage of the plant. Since BvHb1.1 was found to carry a cTP (chloroplast transport peptide) at the N-terminus, it was suggested to be located inside chloroplasts [18].

The role of nsHbs in the regulation of NO in plants has been recognized and widely accepted for a long time [21] and even though mechanisms by which this occurs have been proposed [22] the bimolecular rate constants of the plausible NO reactions remain unknown, even for the species where the role was first proposed, barley [17]. Here, for the first time, we present a thorough biophysical characterization of the three nsHbs with respect to NO and nitrite. Since the localization and expression levels of the three BvHbs is well stablished [18] it is possible to assign a role to each of the three BvHbs, based on their location and their intrinsic reactivity with oxygen, NO, and nitrite.

Hence, here we report a comprehensive and integrated biophysical study of three nsHbs in sugar beet. We have analyzed their reactions with oxygen, CO, NO, and how these are regulated by the coordinating distal histidine. We also evaluate their capacity to carry out NiR and NOD-like functions. The functional implications of these studies are discussed in light of the differential expression of the three BvHbs *in vivo* [18] and the present knowledge on seed germination, and sugar translocation. The results expand our knowledge on the redox chemistry of plant Hbs opening new possibilities for research, breeding and engineering of plants.

Materials and methods

Expression systems

The three sugar beet nsHbs with GenBank Accession No. KF549980 (BvHb1.1), KF549981 (BvHb1.2), and KF549982 (BvHb2) [18] were custom synthesized by Epoch Biolabs (U.S.A.). Recombination-based cloning, and transformation were carried out according to instructions (Gateway™, Invitrogen). The genes were individually cloned into a pET-DEST42 plasmid and the three final expression vectors transformed into BL21-DE3 *E*scherichia *coli* cells.

Growth conditions for expression

Cells containing the expression vectors were grown in sterile TB medium containing 100 μg/ml carbenicillin at 37°C and 150 rpm until $A_{600} \geq 2$. Expression of nsHbs was then induced by adding 0.5 mM IPTG, and 0.3 mM δ-aminolevulinic acid. The cells were also briefly bubbled with CO to obtain a stable CO-BvHb when expressed. After induction, cells were grown overnight at 22°C, 150 rpm, then collected by centrifugation and finally snap-frozen at −80°C until used.

Purification of recombinant BvHbs

All procedures were performed at room temperature and all buffers were pH adjusted. BvHb1.2 and BvHb2 cells were separately resuspended in extraction buffer (50 mM Tris–HCl, pH 8.5, 50 mM NaCl, 25 mM glucose, 1 mM EDTA, 10 μM ascorbic acid, and 5% glycerol, 2 ml per gram of cells). The resuspensions were disrupted by sonication (Q500 Qsonica) and the lysate was clarified twice by centrifugation at 27 000***g***, first 45 min and then 30 min.

An ÄKTA explorer system (GE Healthcare) was used for purification. Recombinant BvHb1.2 was first loaded into a Q-Sepharose FF column and eluted with start buffer (50 mM Tris–HCl, pH 8.5) plus 50 mM NaCl. The red fractions were concentrated using 10 kDa Viva-Spin columns (Vivascience). Ammonium sulfate was then added to the pooled sample to a final concentration of 0.8 M. The sample was then loaded onto a Butyl-Sepharose HP column previously equilibrated with 50 mM Tris–HCl pH 8.0 buffer plus 0.8 M ammonium sulfate. BvHb1.2 was eluted with a 10 CV (column volume) linear gradient ranging from 0.8 to 0 M ammonium sulfate in 50 mM Tris–HCl pH 8.0 buffer. Finally, the protein was loaded onto a Q-Sepharose HP column, and a linear gradient of NaCl from 0 to 100 mM in 50 mM Tris buffer at pH 8.5 was used for elution.

Recombinant BvHb2 was purified in a similar way to BvHb1.2 with some modifications. In the first step, a DEAE-Sepharose FF column was used and the protein was eluted with start buffer plus 200 mM NaCl. In the second step, ammonium sulfate was added to the sample to a final concentration of 0.9 M and the elution was carried out with a 10 CV gradient of 0.9–0 M ammonium sulfate. The final step was the same except that 200 mM NaCl was used to recover the protein.

Since BvHb1.1 carries a leading peptide at the N-terminal region [18], it aggregated when overexpressed. Therefore, after lysis, the aggregated protein was solubilized in 50 mM Tris–HCl pH 8.0, 200 mM NaCl, 6 M Urea, and 1 mM ascorbic acid. The BvHb1.1 solution was then loaded onto a SP-Sepharose FF column pre-equilibrated with start buffer (50 mM Tris–HCl pH 8.0 and 200 mM NaCl) and then eluted with start buffer plus 0.5 M NaCl. The purified nsHbs were analyzed by SDS–PAGE and total heme was determined using the pyridine hemochrome heme assay [23]. They were then flash-frozen in liquid nitrogen and stored at −80°C until needed.

Molecular mass of recombinant nsHbs

The native molecular masses were determined by gel filtration on a HiLoad 16/60 Superdex 200 pg prepacked column (GE Healthcare) using 50 mM sodium phosphate pH 7.2 plus 150 mM NaCl as column buffer and according to the instructions in the Gel Filtration Calibration Kit (GE Healthcare) using the native protein standards: Ferritin (444 kDa), Aldolase (158 kDa), Conalbumin (75 kDa), Ovalbumin (43 kDa), Carbonic anhydrase (29 kDa), RNAse (13.7 kDa), Aprotinin (6.5 kDa). The molecular mass of the monomers of BvHb1.2 and BvHb2 were also determined by mass spectrometry [24].

Bimolecular association rates

The ligand rebinding for CO and oxygen (O_2) to BvHbs was determined by flash photolysis. The apparatus used for the flash photolysis experiments consisted of an Applied Photophysics LKS80 nanosecond flash photolysis spectrophotometer equipped with a xenon light source, dual monochronometers and a Nd:YAG laser. Samples for flash photolysis were prepared as follows: 0.1 M sodium phosphate pH 7.0, was bubbled with either CO or O_2 for 20 min. This solution was then mixed with argon degassed buffer in a separate syringe to generate different CO or O_2 concentrations to be used in each experiment. A solution of 10 μM ferrous BvHb in 0.1 M sodium phosphate buffer pH 7.0, containing an excess of sodium dithionite, was mixed with the solutions of CO (62.5–1000 μM) or O_2 (10–500 μM). Each sample was used to completely fill a glass cell with a 10 mm path length which was sealed with a rubber septum. All rapid mixing experiments were conducted at 20°C. The reactions were followed at 430 and 416 nm or 430 and 410 nm for CO and O_2 binding, respectively.

Carbon monoxide combination rate

Solutions of ferrous BvHb (10 μM) in 0.1 M sodium phosphate pH 7.0 containing an excess of sodium dithionite were rapidly mixed with solutions of CO (25–1000 μM), prepared as above, using an Applied Photophysics SX20 stopped-flow spectrophotometer fitted with a monochronometer photomultiplier or diode array detector interfaced to a PC system. All stopped-flow experiments were carried out at 20°C. The reactions

Biochemical Journal (2019) **476** 2111–2125
https://doi.org/10.1042/BCJ20190154

were followed at 430 and 555 nm, 430 and 560 nm, and 429 and 558 nm for BvHb1.1, BvHb1.2, and BvHb2, respectively.

Oxygen dissociation rate

Two different approaches were used to determine the O_2 dissociation rates. In the first, the displacement of oxygen was determined by rapidly mixing solutions of oxyferrous BvHb with solutions of sodium dithionite (10 and 20 mM). Spectra between 375 nm and 750 nm were recorded using the diode array detector on the stopped-flow over a time course of 50 to 100 s. In the second approach, the replacement of O_2 by CO was carried out by rapidly mixing a degassed solution of BvHb (14 μM) with a solution of CO (500 μM) plus sodium dithionite (20 mM). All experiments were carried out at 20°C using 0.1 M sodium phosphate pH 7.0.

NO binding to ferrous BvHbs

Solutions of ferrous BvHb (10 μM) in 0.1 M sodium phosphate pH 7.0 containing an excess of sodium dithionite were rapidly mixed with Proli NONOate (Cayman chemicals, U.S.A.). A stock solution (80 mM) was freshly prepared by dissolving 10 mg of Proli NONOate in 1 ml of degassed NaOH (25 mM) and kept on ice (0°C) where it is stable for 24 h. The stock was diluted just before mixing and the NO concentration ranged from 800 to 25 μM. The reactions were followed monochromatically (426 nm) at 15°C for BvHb1.2 and 20°C for BvHb1.1 and BvHb2. The stopped-flow spectrophotometer used was described above.

NO dioxygenase-like activity

The described above stopped-flow spectrophotometer was used to analyze the stoichiometric reaction between oxyferrous BvHbs and NO at 10°C. Solutions of oxyBvHb (10 μM) in 100 mM sodium phosphate buffer pH 7.0 were rapidly mixed with Proli NONOate (80, 40, and 26 μM for BvHb1.1), prepared as described in the experiment above. The reactions were followed monochromatically at 408 nm for BvHb1.1 and BvHb1.2, and 430 nm for BvHb2.

Nitrate reductase activity

Nitrate reductase activity was assessed under anaerobic conditions using a method previously described [25] in which 10 μM ferrous BvHb (in NaP 100 mM pH 7.0) plus 10 mM sodium dithionite was mixed with solutions of $NaNO_2$ (from 25 to 200 mM) at 20°C. Reaction progress was monitored by observing absorbance changes at 426 nm.

Data analysis

In all cases, at least three kinetic traces were collected and averaged. The data were analyzed using the Applied Photophysics Pro-K II global analysis software except when having single wavelength data (stopped-flow and flash photolysis). In that case, it was analyzed using the Applied Photophysics ProData SX software. The OriginPro program (OriginLab) was employed for the generation of figures.

Results

Characterization and heme iron coordination of BvHbs

BvHbs were purified from *E. coli* crude cell extracts. SDS–PAGE of the protein revealed bands of 27.0, 17.0, and 15.0 kDa for BvHb1.1, BvHb1.2, and BvHb2, respectively (Supplementary Figure S1A). Native molecular masses as assessed by mass spectrometry and size-exclusion chromatography on Superdex 200 were determined to be 53.0, 38.6, and 17.5 kDa for BvHb1.1, BvHb1.2, and BvHb2, respectively (Figure 1 and Supplementary Figure S1B). Therefore, it is concluded that both class-1 BvHbs are homodimers, as previously shown for other class-1 nsHbs [26,27] and that BvHb2 is a monomer.

The three purified proteins displayed spectra typical of ferrous low spin species having bis-histidyl heme coordination, indicating that their heme group is hexacoordinated like other nsHbs (Figure 1) [6–8]. Reactions of hexacoordinated proteins with ligands are strongly influenced by the association and dissociation rate constants of the distal histidine residue (Scheme 1) [28,29]

$$\mathrm{Hb_{hex}} \underset{k_H}{\overset{k_{-H}}{\rightleftharpoons}} \mathrm{Hb_{pent}} + \mathrm{L} \underset{k_L}{\overset{k'_L}{\rightleftharpoons}} \mathrm{Hb_L} \qquad \text{(Scheme 1)}$$

Biochemical Journal (2019) **476** 2111–2125
https://doi.org/10.1042/BCJ20190154

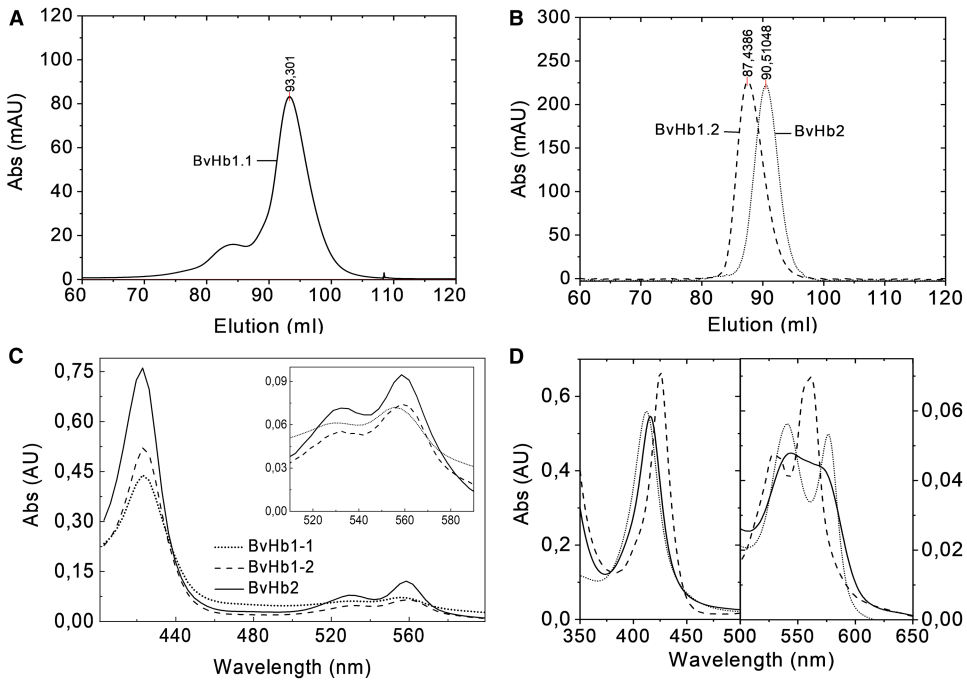

Figure 1. NsHbs in sugar beet.

Size exclusion chromatography (**A**) BvHb1.1 (53 kDa) eluted at 93.3 ml, nearest standards eluted at 84,69 (conalbumin, 75 KDa) and 96,9 ml (carbonic anhydrase, 29 KDa). (**B**) BvHb1.2 (38.6 KDa) and BvHb2 (17.5 KDa) eluted at 87,4 ml and 90,5 ml, respectively. The nearest standards eluted at 80,5 (conalbumin, 75 KDa) and 96 ml (RNAse A, 13.7 KDa). (**C**) The three BvHbs display spectra of ferrous low spin species typical of bis-histidyl forms after sodium dithionite addition. *Inset*, α and β peaks at the visible region. (**D**) Absorbance spectra of BvHb1.2 in its oxy- (*dotted line*), deoxy- (*dashed line*), and NO-form (*line*).

A common approach to determine the rate constants for distal histidine coordination (H) and exogenous ligand (L) binding of hexacoordinated proteins is by investigating their CO binding kinetics. Assuming that the concentration of Hb_{pent} remains small and in a steady-state and that k_{CO} is very small, results in eqn 1 where $k_{obs.CO}$ is the observed rate constant of CO binding to the hexacoordinated state of the protein [28]:

$$k_{obs,CO} = \frac{k_{-H}k'_{CO}[CO]}{k_H + k_{-H} + k'_{CO}[CO]} \quad (1)$$

Eqn 1 allows the determination of rate constants for hexacoordination (k_H and k_{-H}) by using $k'_{CO.pent}$ which is determined independently from flash photolysis experiments.

CO binding by stopped-flow rapid mixing

On rapidly mixing CO with any of the three BvHbs, a single exponential process was observed accounting for >90% of the absorbance change. The spectra associated with these single exponential processes conform to that expected from static spectra namely the formation of the CO adduct from the ferrous hexacoordinate species (Figure 2A and Supplementary Figure S2). The rate constant (k_{obs}) for this transition exhibited a hyperbolic dependance on CO concentration (Figure 2B). The asymptotic values approached at high CO concentrations depended on the protein under study and they were 118.7 s^{-1}, 47.4 s^{-1}, and 48 s^{-1} for BvHb1.1, BvHb1.2, and BvHb2, respectively (Table 1). These data are consistent with CO-binding to the hexacoordinated form limited by the dissociation rate constant of the intrinsic distal histidine ligand (Scheme 1).

Laser flash photolysis

The CO rebinding kinetics of the three proteins, after photo-dissociation, are shown in Figure 3. Here, the time courses were fitted to double exponential functions (Figure 3A). The fast phase representing the binding of CO

Biochemical Journal (2019) **476** 2111–2125
https://doi.org/10.1042/BCJ20190154

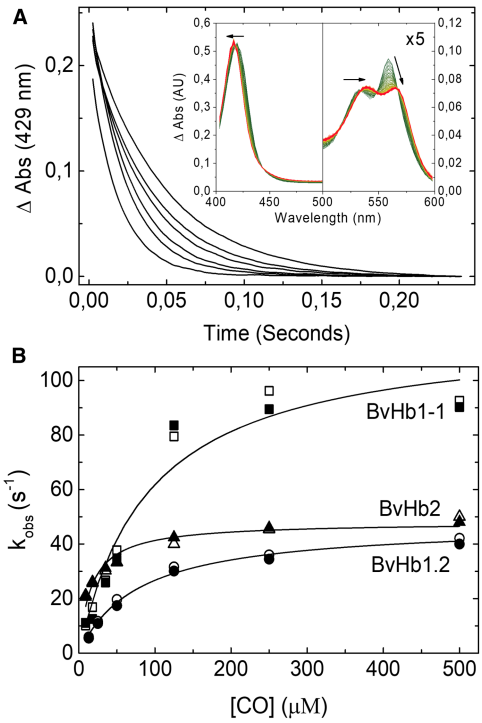

Figure 2. CO binding to BvHbs by stopped-flow rapid mixing.

(**A**) Time courses for CO binding to BvHb2 following rapid mixing at different CO concentrations (from left to right: 500, 250, 125, 35, 18, and 9 μM) monitored at 429 nm. *Inset*, Absorbance spectra associated with the binding of CO to ferrous BvHb2. The direction of the spectra changes from deoxyHb (green) to HbCO (red). (**B**) CO dependance of the rate constants for binding to the three BvHbs determined by stopped-flow rapid mixing. The data are fitted to eqn 1 to extract the hexacoordination rates, k_H and k_{-H}. The closed and open symbols are k_{obs} values monitored at 430 and 555 nm for BvHb1.1, 430 and 560 nm for BvHb1.2, and 429 and 558 nm for BvHb2.

to the transient pentacoordinate form generated by photolysis and the slow process representing the CO binding to the hexacoordinate species formed by histidine rebinding to the iron (Figure 3B). The rebinding kinetics of BvHb1.1 and BvHb1.2 may adequately be described by Scheme 1. This is observed in the CO-dependent curves obtained by stopped-flow and the slow phase of rapid mixing which are, as expected, comparable.

However, BvHb2, while exhibiting a fast phase corresponding to CO binding to the pentacoordinate form, displayed a slow phase the CO concentration dependance of which was significantly faster than that given by stopped-flow spectrometry (Figure 3C). This phenomenon has also been described by Trent et al. [30] who accounts for the discrepancy by proposing that the hexacoordinate form populated following flash photolysis (termed 'open', $Hb_{O,H}$) is metastable and at longer times relaxes to the closed hexacoordinate form (termed 'closed', Hb_C) that is studied in stopped-flow experiments. Given this model, the limiting rate constant seen at high [CO] in stopped-flow experiments is that for the transition from the stable ferrous form (Hb_C) (Figure 2B) while that for the slow phase following photolysis gives the histidine off rate (k_{-H}) from the meta-stable state ($Hb_{O,H}$) (Figure 3C). The correspondent $k_{H,}$ and k_{-H}, and K_H (k_H/k_{-H}) were calculated for both ferrous forms (Table 1).

The pseudo first-order constants for CO rebinding to the pentacoordinate form following flash photolysis are shown in Figure 3B. The slopes of these plots yield the bimolecular rate constants for CO rebinding to the deoxyHb intermediate ($k'_{CO,pent}$): 3.68×10^6, 1.27×10^6, and 17×10^6 M^{-1} s^{-1} for BvHb1.1, BvHb1.2, and BvHb2, respectively. Both class-1 BvHbs had lower bimolecular CO binding rates than BvHb2 in agreement with values reported for other plant Hbs [3].

The hexacoordination values for the three sugar beet Hbs (Table 1) were calculated through analysis of the hyperbolic curves (Figure 2) obtained from stopped-flow experiments together with independently determined values of k'_{CO}. An alternative method has been reported in which either the sum or multiple of the two pseudo

Biochemical Journal (2019) **476** 2111–2125
https://doi.org/10.1042/BCJ20190154

Table 1 Ligand binding and hexacoordination rates for different plants Hbs.

	$k'_{O_2\ pent}$[1]	k_{O_2}[2]	$K_{O_2\ pent}$[3]	K_{O_2}[4,3]	$k'_{CO\ pent}$[1]	k_H[2]	k_{-H}[2]	K_H	F_H[5]	References
Class-1 Hbs										
AtHb1	74	0.12	617	200	0.55	230	110	2.1	0.68	[3, 8]
BvHb1.1	59	0.075	787	271	3.68	220	118	1.9	0.66	This study
BvHb1.2	57	0.158	361	157	1.27	59.5	47.4	1.3	0.57	This study
Tomato Hb1	30	0.5	60	30	1	200	200	1	50	[45]
Soybean Hb1	59	0.013	4538	1512	2.7	160	80	2	0.67	[3]
Lotus Hb1-1	81	0.004	20250		1.2	67	27	2.48	0.71	[46, 47]
Lotus Hb1-2	300	0.27	1111		29	1484	88	16.9	0.94	[46, 47]
Barley Hb1	50	0.027	1852	440	2	170	62	2,8	0.74	[48]
Maize 1a	44	0.054	820	430	1.4	22	25	0.9	0.47	[28]
Maize 1b	210	0.27	780	240	44	43	19	2.3	0.69	[28]
RiceHb1a	60	0.038	1579	540	6.8	75	40	1.9	0.65	[6, 49]
RiceHb1b	40	0.1	400	280	1.8	6.7	15	0.45	0.31	[49]
Class-2 Hbs										
AtHb2	86	0.14	614	21	77	330	12	28	0.96	[8, 50]
BvHb2	72	0.094	766	132, 551[6]	17	232	48, 600*	4.8, 0.39*	0.83, 0.28*	This study
Chicory 2a	50	0.11	455	1.7	54	2900	11	264	0.99	[3]
Chicory 2b	50	2.7	19	0.5	10	920	27	34	0.97	[3]
Tomato Hb2	45	0.4	113	1.9	26	1400	30	47	0.98	[3]
Lotus Hb2	77	0.86	90		3,79, 10,71*	0.033, 4.4*	0.15, 20*	0.22	0.18	[46, 47]

Eudicot plants (light blue). Eudicot plants that also have sHbs (dark blue). Monocot plants (green).
[1]$\times 10^6\ M^{-1}\ s^{-1}$;
[2]S^{-1};
[3]$\times 10^6\ M^{-1}$;
[4] $K_{O_2,pent}/(1+K_H)$;
[5] $F_H = K_H/(1+K_H)$;
[6]Rate constants for the metastable form ($Hb_{O,H}$).

first-order rate constants observed in photolysis experiments are plotted against [CO] [29]. Determining the slopes and intercepts of these linear plots (not shown) provide a way to calculate the values of the parameters defined in Scheme 1. We have applied this method to our data. For BvHb1.1 we obtained values for k_H and k_{-H} broadly in agreement with those given in Table 1. For BvHb2 this analysis returned values of 539 s^{-1} and 113 s^{-1} for k_{-H} and k_H, respectively. We have already commented above that this protein appears to behave as described by Trent et al. [30] and after photolysis of the carboxy-adduct populates a metastable 'open' structure, different in conformation from the stable ferrous form but still retaining histidine coordinated to the iron as in the 'closed' ferrous structure. Given this, the k_{-H} value of 539 s^{-1} may be taken as the histidine dissociation rate constant for the 'open' ferrous form. If also the 'closed' structure is not (or little) populated following photolysis then the 113 s^{-1} value may be taken as the histidine association rate constant in the 'open' form. Treating the data obtained for BvHb1.2 by Scheme 1 however lead to inconsistent results. The value found for k_{-H} was 65.7 s^{-1}, in reasonable agreement with the value, 47.4 s^{-1} given in Table 1, but the value for k_H became negative, clearly incorrect. The reason for anomalous result is not presently clear but the simplest explanation may be that the value of the intercept on the plot of the sum of the two rate constants against [CO] has been underestimated owing to error in the [CO] but this seems unlikely given the consistency of the other results. Rather it may arise from the fact that the simplest model (Scheme 1) and assumptions do not apply to BvHb1.2. For example, if the model required to describe BvHb1.2 needs more steps and thus includes further intermediates than the two-step model we may expect the method to breakdown. We have not so far seen evidence of such intermediates but their presence may not be obvious if the rate constants for their

Biochemical Journal (2019) **476** 2111–2125
https://doi.org/10.1042/BCJ20190154

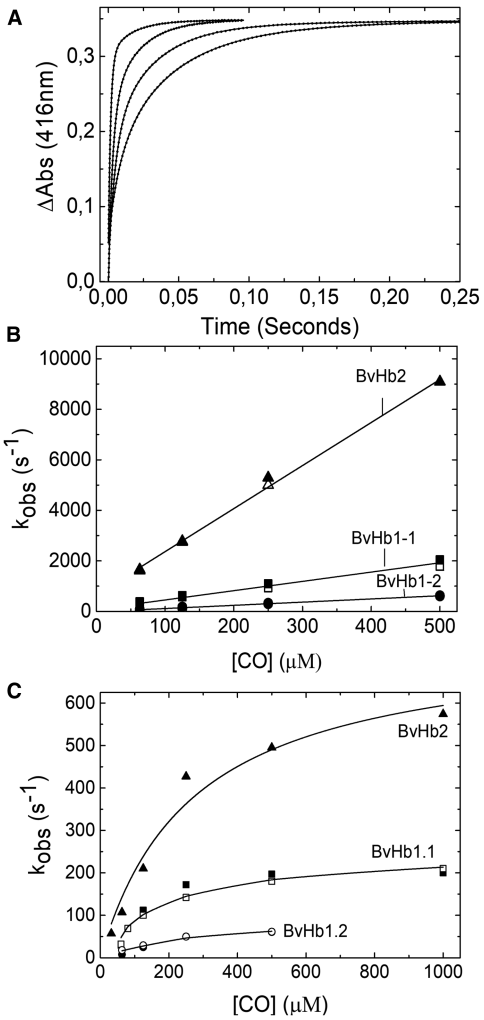

Figure 3. CO binding to BvHbs by flash photolysis.

(**A**) Time courses for rebinding of CO to BvHb1.2, after flash photolysis, monitored at 416 nm. The binding is a double exponential process at all CO concentrations (from left to right: 500, 250, 125, and 63 μM). (**B**) Fast phase and (**C**) Slow phase of the rebinding of CO to the three BvHbs. For BvHb1.1 and BvHb1.2 (both class-1) the approximate rates of the slow phase are essentially the same as reported by stopped-flow (Figure 2B). For BvHb2, this slow phase is faster than the value given by stopped-flow spectrometry. The closed and open symbols correspond to k_{obs} values monitored at 429 nm for BvHb2 and 416 nm and 430 nm for BvHb1.1 and BvHb1.2.

formation and decay are such that these are close in value to the first-order rate constants k_{-H} and k_H and each other. Further experiments are required to resolve this problem.

Oxygen binding and dissociation

The association of oxygen to BvHbs could not be estimated using stopped-flow spectroscopy because this technique is limited by relatively long mixing dead times. However, the oxygen-iron bond is photo labile and recombination of oxygen with the pentacoordinate heme, following laser photolysis, may be tracked and the second-order association rate constants thus determined.

Following photo-dissociation of the oxy-complex, a single exponential rate was observed for rebinding of oxygen to the three BvHbs (Figure 4A and Supplementary Figure S3). The pseudo first-order constants for oxygen rebinding as a function of O_2 concentration are shown in Figure 4B. The slopes of these plots yield the bimolecular rate constant for oxygen rebinding to the pentacoordinate Hb ($k'_{O_2,pent}$ in Table 1).

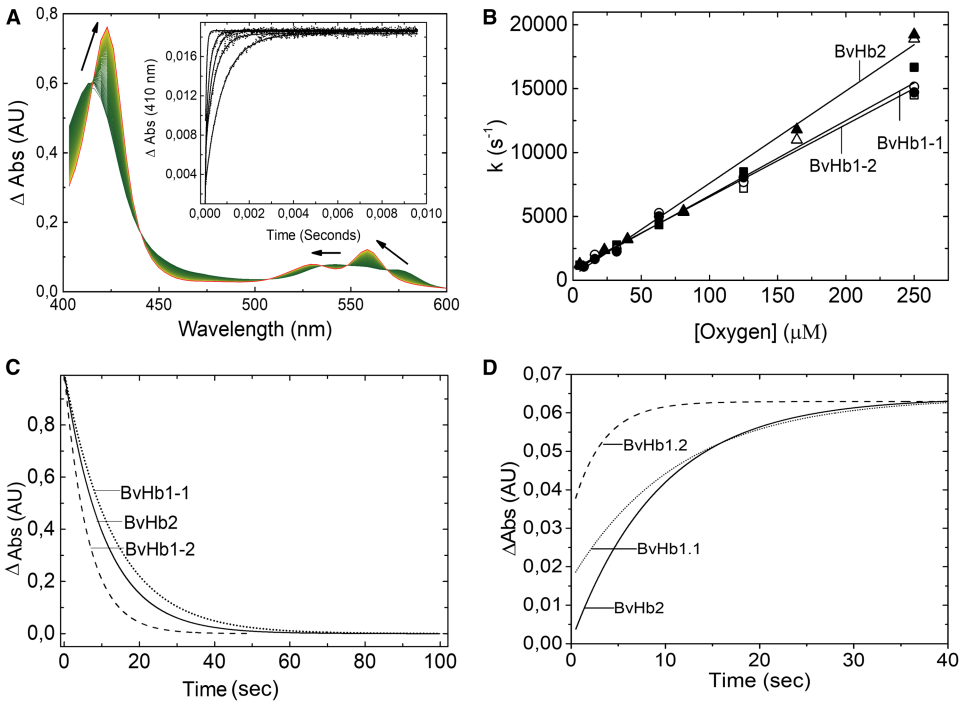

Figure 4. Oxygen binding to BvHbs.

(**A**) Absorbance spectra associated with the binding of oxygen to deoxygenated BvHb2. The direction of the spectra changes from deoxyHb (green) to oxyHb (red). Inset: Time courses for rebinding of oxygen after flash photolysis at different oxygen concentrations (from left to right: 250, 81, 39, 23, and 5 μM) monitored at 410 nm. (**B**) Dependances of the pseudo first-order ligand rebinding rates on different oxygen concentrations, as measured by flash photolysis, provide k'O_2 values. The closed and open symbols correspond to k_{obs} rates monitored at 410 and 430 nm, respectively. Time courses for the dissociation of oxygen after the addition of sodium dithionite (**C**) and when oxygen is replaced by CO (**D**).

On rapidly mixing each of the proteins with the only dithionite or with dithionite plus CO, a single homogeneous kinetic event, independent of sodium dithionite and CO concentrations was obtained for the three proteins (Figure 4C,D). The spectra associated with this kinetic event with dithionite or with dithionite plus CO conformed to that expected for the transition from oxy- to deoxy-Hb (Supplementary Figure S3) and from oxy to CO-Hb, respectively. Time courses were fitted to a single exponential curve. The dissociation constant rates (k_{O_2}) obtained when mixing sodium dithionite with oxy Hb were equal to the rates obtained when CO was used to replace O_2. The obtained (k_{O_2}) for BvHb1.1, BvHb1.2 and BvHb2 were 0.075, 0.158, and 0,094 s^{-1}, respectively (Table 1).

The affinity of each of the BvHbs for oxygen (K_{O_2}) was determined using the values of K_H given in Table 1 together with eqn 2 [3]:

$$K_{O_2} = \frac{K_{O_2.\,pent}}{1 + K_H} \quad (2)$$

The $K_{O_2.\,pent}$ represents the affinity to the pentacoordinate form and was estimated from the ratio of the second-order rate constant for oxygen rebinding following flash photolysis to the rate constant for oxygen dissociation determined by stopped-flow experiments using sodium dithionite as an oxygen scavenger.

NO binding to deoxyferrous BvHbs

On mixing the deoxy proteins with NO, rapid binding absorbance changes were seen correspondent to expectation for the formation of deoxy-nitrosyl complex (Figure 5A). The pseudo first-order rate constants (k_{obs}) for NO binding for the three proteins are shown as a function of NO concentration in Figure 5B. These data show

Biochemical Journal (2019) **476** 2111–2125
https://doi.org/10.1042/BCJ20190154

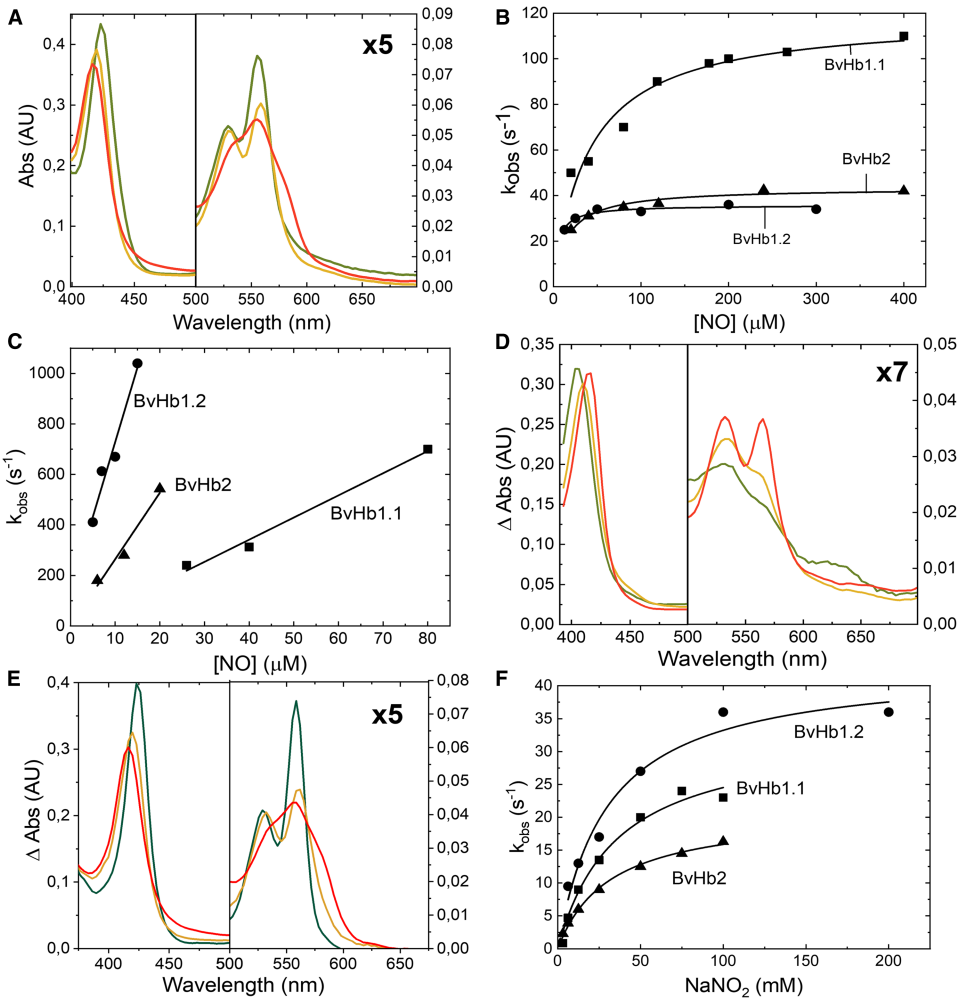

Figure 5. NO and nitrite reaction with BvHbs.

(**A**) Fitted spectra changes associated with the addition of NO to deoxyferrous BvHb1.2 (from green to red). (**B**) Pseudo first-order rate constants (k_{obs}) for NO binding for the three proteins are shown as a function of NO concentration. (**C**) Rate constants for the dioxygenase reaction was found to be linearly dependent on NO concentration for the three BvHbs. (**D**) Fitted spectra changes associated with the production of ferric Hb-NO adduct (from green to red) after the NOD reaction. (**E**) Fitted spectra changes associated with deoxyferrous BvHb1.2 following the addition of sodium nitrite. (**F**) The rate constants for nitrite reduction are plotted as a function of sodium nitrite concentrations resulting into hyperbolas. The k_{obs} values are taken to be the His_{off} rate constant as found with the CO and NO experiments.

that k_{obs} in each case approaches a limiting value indicating that NO binding is limited by His_{off} (K_{-H}) as seen for CO binding. These His_{off} rates are 118 s^{-1} and 44 s^{-1} for BvHb1.1 and BvHb2, respectively. In the case of BvHb1.2 it is slightly lower (36 s^{-1}) which is to be expected as it was determined at lower T°. Fits to these data to eqn 1 also give estimates for the NO binding rate constants to the pentacoordinate form of the three BvHbs (Table 2).

NO dioxygenase-like activity

Estimates of NOD-like activity, followed through the production of the ferric protein, were obtained by mixing the oxyBvHbs with NO at 10°C. Rate constants for these processes were found to be linearly dependent on NO concentration (Figure 5C) and yielding second-order rate constants for the three BvHbs (Table 2). Following oxidation of the heme, a series of slower reactions occur as reported by others that reflect NO_3^- escape from the heme cavity and binding of NO to the ferric form (Figure 5D). The rates at which the ferric Hb-NO adduct is

Biochemical Journal (2019) **476** 2111–2125
https://doi.org/10.1042/BCJ20190154

Table 2 Kinetic values for reactions of plants Hbs with NO and nitrite

	$k'_{\text{No pent}}$ [1]	k_{NOD} [1]	k_{NiR} [2]	$k'_{\text{Fe}^{+3}\text{–NO}}$ [3]	References
BvHb1.1	8.1	8.8	5.3	2.8	This study
BvHb1.2	17	59.1	3.1	0.5	This study
AtHb1			58		[11,32]
RiceHb1			83		[12]
BvHb2	15.5	26.3	8.3	0.3	This study
AtHb2			11		[11,32]

[1] $\times 10^6\ M^{-1}\ s^{-1}$.
[2] $\times 10^3\ M^{-1}\ s^{-1}$;
[3] s^{-1}.

formed differs among the BvHbs. These rates were 2.8 s^{-1}, 0.5 s^{-1}, and 0.3 s^{-1} for BvHb1.1, BvHb1.2, and BvHb2, respectively.

Nitrite reductase activity

The reaction mechanism is shown in Scheme 2, and the end product is Fe(II)-NO (Figure 5E) [31]. Since the generated NO has a very high affinity for the ferrous heme, as demonstrated above, the final product of the reaction will be iron-nitrosyl-heme [Fe(II)-NO] [11].

$$\text{FeII} + NO_2^- \xrightarrow{2H^+,\ H_2O} \text{FeIII·NO} \xrightarrow{\text{Dithionite}} \text{FeII·NO} \qquad \text{(Scheme 2)}$$

We found that at high concentrations of dithionite the second reaction may be fast and thus the intermediate ferric species may not be seen. In order to assure ourselves of the mechanism we undertook experiments using low dithionite concentrations (but still in excess over the protein concentration). Under those conditions we indeed observed the ferric-NO form, proving the first step of the mechanism was taking place and eliminating the possibility that contaminant NO, possibly resulting from the reaction of nitrite with dithionite, was binding to the heme. Had this been the case, no ferric intermediate would have been observed but rather an immediate production of the ferrous NO species. The stopped-flow experiment, analyzed in terms of a sample sequential model, shows the initial ferrous form converted to the ferric-NO form proving a nitrite reductase activity and then to the ferrous NO form (Figure 5E and Supplementary Figure S4D). The intermediate may be assigned unequivocally as the ferric-NO form by comparing it with the static spectra obtained on adding NO to the ferric protein (Supplementary Figure S4A–C).

Having confirmed that a true NiR activity is present, the remaining stopped-flow experiments reported here were performed at high dithionite as described before [25]. On mixing the ferrous proteins with NO_2^- biphasic reactions were observed. The faster process we assign is the binding of nitrite and production of the ferrous NO complex (at high dithionite concentration the ferric intermediate is not seen). The rate constant (k_{obs}) for the NiR activity may be seen plotted against $NaNO_2$ concentration for each of the three proteins in Figure 5F. The rate constants tend towards the plateau and each data set may be fitted satisfactorily to a hyperbola (eqn 1). These fits yield the maximum value for k_{obs} 39 s^{-1}, 43 s^{-1}, and 20 s^{-1} for BvHb1.1, BvHb1.2, and BvHb2, respectively, which in keeping with the other ferrous ligands, we take to be the His_{off} rate constant. Although this is likely to be the case, we note that the values of His_{off} determined from the nitrite experiments are lower than those found for the CO and NO experiments. These differences are probably due to the requirement of the proximal His to move further away from the heme group to allow the larger and charged nitrite ion access to the heme. Such requirements may well be reflected in an apparently lower His_{off} rate. This effect is more apparent in BvHb1.1 and BvHb2 than in BvHb1.2. The fits in Figure 5F also allow estimates to be made of binding rate constants for nitrite (NO_2^-) which are given in Table 2. The results indicate that the entrance of nitrite to the heme pocket is less limited in BvHb2. As a result, BvHb2 has a bimolecular rate constant around 2-fold higher than class-1 BvHbs. When these results are compared with those reported for

Biochemical Journal (2019) 476 2111–2125
https://doi.org/10.1042/BCJ20190154

Arabidopsis and rice nsHbs (Table 2), the NiR activities of the three BvHbs are up to 90- and 700-fold higher than their class-1 and class-2 counterparts, respectively.

Discussion

Beta vulgaris ssp. *Vulgaris*, sugar beet, is a species the physiology of which has been widely studied owing to its economic significance. In order to get a better insight into the role of its three non-symbiotic Hbs (BvHbs), we investigated their binding properties with regard to endogenous and exogenous ligands. The results obtained are discussed in the light of sugar beet physiology and the known and differing expression profiles of the three BvHbs that are specific in term of organs and developmental stage [18].

Our results, together with data from other plant species, suggest that the affinity of nsHbs for oxygen ($K_{O_2,pent}$) is closely related to the phylogeny and evolution of plants. Currently, class-1 Hbs are reported to have a higher affinity for oxygen than class-2 Hbs. We found, however, that this conclusion is not justified if the taxonomy of plants is taken into account. It is apparent that class-1 nsHbs from eudicot plants have oxygen affinities that are not very different from the estimated values for class-2 nsHbs ($456 \times 10^6 \pm 3.17 \times 10^2$ and $343 \times 10^6 \pm 3.12 \times 10^2$ M^{-1}, respectively) ($K_{O_2,pent}$), Table 1). Interestingly, we note that it is the class-1 nsHbs from leguminous plants that have the highest oxygen affinity ($8600 \times 10^6 \pm 10.2 \times 10^3$ M^{-1}). These are then followed by the values of monocot plants ($1080 \times 10^6 \pm 6 \times 10^2$ M^{-1}). Therefore, the current view on plant nsHbs, where class-1 nsHbs are attributed to have a higher affinity for oxygen than class-2 needs to be reassessed. Such conclusion is misleading and should be modified by stating instead that class-1 nsHbs from legumes and monocots have higher oxygen affinity (3- to 25-fold) than class-1 and class-2 nsHbs from eudicot plants.

The influence of hexacoordination on ligand binding is clearly observed in the reactions with oxygen, CO, and NO. Our results show how important K_H is for the binding of exogenous ligands. The oxygen association and dissociation rate constants for the pentacoordinate forms of all three proteins are very similar, within a factor of two (Table 1). However, it is the high K_H value that reduces the overall affinity of BvHb2 (Hb_C) for oxygen ~6-fold. The net result of stronger hexacoordination is that class-2 nsHbs have P_{50} values for oxygen binding similar to mammalian Mbs, which are roughly 200-fold greater than class-1 nsHbs and ~10-fold greater than sHbs [3]. In the case of BvHb1.1 and BvHb1.2 their low K_H reduces their affinity for oxygen for just ~2- or 3-fold. The role of distal histidine as a limiting factor for the binding of CO and NO is also clearly observed in our results. The k_{obs} in each case approach a limiting value indicating that NO and CO binding is limited by His_{off} (Figures 2B and 5B).

When comparing CO binding, the rate constants of binding to pentacoordinate BvHb2 is roughly 5–10 times faster than to both class-1 BvHbs, indicating that the iron accessibility of this protein is much greater. This intrinsic reactivity seems to be the result of both its high histidine dissociation rate and its high hexacoordination fraction. That means that the iron-HisE7 geometry in class-2 proteins is more favorable for ligand binding but, as with oxygen, its overall affinity is lowered by stronger hexacoordination with the distal histidine.

The reaction of nitrite with BvHbs is also affected by their hexacoordination. Our results show that both class-1 BvHbs have between 1.5- to 3-fold lower NiR activities than BvHb2. This result agrees with another study where a pentacoordinate mutant AtHb1 had a much lower NiR activity than a hexacoordinated mutant AtHb2 [32] but contradicts studies in which it was concluded that the NiR activity is higher in Hbs having more pentacoordinate form i.e. lower F_H [11,33]. The disagreement can be due to the distinct environment within the heme pocket and its interaction with the ligand. The effect of such interaction was observed on the His_{off} values which were lower when the ligand was nitrite compared with the values obtained with CO and NO.

The three BvHbs studied here bind NO both in their ferrous and ferric form, they can also reduce nitrite in their deoxy forms to produce NO, and in their oxy forms they can oxidize NO to form nitrate. All these at very distinct rates. Although we cannot confidently assign them cellular functions from consideration solely of their biophysical/biochemical properties, it is plausible to propose such functions in the light of these properties and knowledge of their cellular location and expression profiles. Below we put forward proposals for the cellular roles of each BvHb.

BvHb1.2 is only expressed in seeds of sugar beet [18]. These seeds are unusual in the sense that they are surrounded by a protective layer called pericarp. The pericarp serves as the main storage reservoir for nitrate, ammonium and α-amino-N [34]. Since the uptake of external nitrate depends entirely on the actual internal nitrate concentrations, nitrate must be produced by the seed. As demonstrated in this work, nitrate is swiftly

produced by BvHb1.2 from NO and oxygen (Table 2). The improved root and shoot growth observed in seedlings treated with a NO donor (SNP) [35] support the role of BvHb1.2 as a NOD. Thus, we suggest that BvHb1.2, thanks to its high NOD-like activity, contributes to the creation in the pericarp of a microenvironment adapted to allow the seedling autonomous growth for 8–10 days after imbibition [34].

A proteomics study has demonstrated that seeds of sugar beet possess mitochondrial and plastid protein addressing systems [36] supporting the presence of BvHb1.1 in seeds which needs to be translocated into chloroplasts [18]. Furthermore, the expression of BvHb1.1 increases by 3-fold in hypocotyls concurring with the end of germination (marked by radicle emergence) and greening process characterized by chloroplast biogenesis [18,37]. Further studies suggest that NO is produced in chloroplasts and that it has a positive role in greening process and hypocotyl formation [38,39]. Since the bimolecular rate constants for NO binding and nitrate formation are not so distinct, it is highly probable that BvHb1.1 modulates NO levels inside the chloroplast in order to avoid its deleterious effects [37]. First, at the very beginning of germination, by binding NO in the absence of oxygen, and later by forming nitrate once the seeds' operculum opens and gas exchange and oxygen level improve [40–42]. Furthermore, the additional nitrate produced by BvHb1.1 would induce a rapid hypocotyls extension as observed with seedlings treated with external nitrate [34].

Our results show that BvHb2 is highly reactive towards gaseous ligands binding oxygen and CO rapidly (Table 1). It is also able to adopt two different conformational states, stable and metastable, suggesting that BvHb2 is a dynamic protein. This protein is the most expressed Hb in sugar beet and its presence is ubiquitous in all stages of the plant, except seeds. BvHb2 is almost constitutively expressed in leaves where its response to vernalization and photoperiod coincides with the response of carbon allocation and carbohydrate metabolism [18]. A recent transcriptomic study found that carbohydrate metabolism was the most represented and regulated pathway when wax apple was treated with NO [43] but the underlying molecular mechanisms have not yet being investigated. An investigation of a possible role for BvHb2 in regard to carbon metabolism/allocation and NO seems fully worthwhile. It is likely that BvHb2 is regulating NO levels but given the results in this work, in the presence of oxygen and NO, nitrate would be the main product if BvHb2 is promptly reduced.

Turning to the NiR activity, our results show that the reaction with nitrite is at least thousands fold slower than with NO; therefore, the NiR activity of nsHbs, particularly BvHbs, would be relevant for oxygen balance and NO generation only when nitrite concentrations are at mM levels and when both NO and oxygen are low or absent. In plants, a cellular environment characteristically low in oxygen is found in seeds. Borisjuk et al. [44] observed *in vitro* that seeds reduced their oxygen uptake as a response to the increase in NO produced from nitrite, as a result seeds avoided to fall into anoxia. Other studies have also shown that nsHbs are adept at reducing nitrite to NO under anaerobic conditions and low pH [11,12], conditions that are both met in seeds. In seeds of sugar beet, BvHb1.2 is fully capable to reduce nitrite, but as already noted, this activity would be significant when the seeds are close to anoxia.

Finally, we observed that in the absence of a reductant, the three BvHbs are able to bind NO in their ferric form. We put forward the idea that this Ferric-NO form could enact as a signal molecule within a NO sensing mechanism to detect excessive NO levels in the cell. However, more research on this topic needs to be done in order to validate this idea.

In conclusion, the three proteins have distinct intrinsic capabilities to carry out diverse enzymatic reactions; but their location and the appropriate concentration of oxygen, NO, and nitrite will determine their activity. Thus, the role of BvHb1.2 as a NOD-like within the seed is plausible given the high rate at which nitrate is produced. BvHb1.1, in contrast, seems to be equally equipped to bind NO or to act as a NOD, in any case, the main role would be to protect the chloroplast from NO, and how this is achieved needs further investigation. Finally, the capacity of BvHb2 to adopt 'open and closed forms' depending on ligand concentration confers reactivity and enzymatic versatility to this protein. Since its ubiquitous expression coincides with vernalization and carbon allocation behavior we postulate the existence of an oxygen concentration-dependent relation between NO, BvHb2, and carbon metabolism. In conditions such vernalization and flowering, when oxygen is indispensable for carbon allocation, BvHb2 may help to maintain ATP levels, energy changes, and prevent the onset of cell death, but it is a hypothesis that needs to be proven.

Abbreviations

CO, carbon monoxide; Hb, hemoglobin; NiR, nitrite reductase; NO, nitric oxide; NOD, nitric oxide dioxygenase; nsHb, non-symbiotic hemoglobin; sHb, symbiotic hemoglobin; SNP, sodium nitroprusside; trHb, truncated hemoglobin.

Biochemical Journal (2019) **476** 2111–2125
https://doi.org/10.1042/BCJ20190154

Author Contribution

N.L.E., M.T.W., and L.B. designed the research; N.L.E., M.T.W., and B.J.R. performed the research; N.L.E.; M.T.W., and B.J.R. analyzed the data. N.L.E. and M.T.W. wrote the main body of the manuscript while B.J.R. and L.B. significantly contributed to the discussion and the article's completion. All authors have read and approved the final manuscript.

Funding

Funding was provided by the Royal Physiographic Society of Lund [Grants 26563, 31587], the Swedish Research Council for Environment, Agricultural Sciences and Spatial Planning (Formas 2016-00902), the Swedish Foundation for Strategic Research [RBP14-0055], and the Swedish Research Council [VR 5607-2014].

Competing Interests

The Authors declare that there are no competing interests associated with the manuscript.

References

1 Vazquez-Limon, C., Hoogewijs, D., Vinogradov, S.N. and Arredondo-Peter, R. (2012) The evolution of land plant hemoglobins. *Plant. Sci.* **191–192**, 71–81 https://doi.org/10.1016/j.plantsci.2012.04.013
2 Vinogradov, S.N. and Moens, L. (2008) Diversity of globin function: enzymatic, transport, storage, and sensing. *J. Biol. Chem.* **283**, 8773–8777 https://doi.org/10.1074/jbc.R700029200
3 Smagghe, B.J., Hoy, J.A., Percifield, R., Kundu, S., Hargrove, M.S., Sarath, G. et al. (2009) Review: correlations between oxygen affinity and sequence classifications of plant hemoglobins. *Biopolymers* **91**, 1083–1096 https://doi.org/10.1002/bip.21256
4 Hill, R., Hargrove, M. and Arredondo-Peter, R. (2016) Phytoglobin: a novel nomenclature for plant globins accepted by the globin community at the 2014XVIII conference on oxygen-binding and sensing proteins. *F1000Res.* **24**, 212 https://doi.org/10.12688/f1000research.8133.1
5 Hunt, P.W., Watts, R.A., Trevaskis, B., Llewelyn, D.J., Burnell, J., Dennis, E.S. et al. (2001) Expression and evolution of functionally distinct haemoglobin genes in plants. *Plant Mol. Biol.* **47**, 677–692 https://doi.org/10.1023/A:1012440926982
6 Arredondo-Peter, R., Hargrove, M.S., Sarath, G., Moran, J.F., Lohrman, J., Olson, J.S. et al. (1997) Rice hemoglobins. Gene cloning, analysis, and O_2-binding kinetics of a recombinant protein synthesized in *Escherichia coli*. *Plant Physiol.* **115**, 1259–1266 https://doi.org/10.1104/pp.115.3.1259
7 Duff, S.M., Wittenberg, J.B. and Hill, R.D. (1997) Expression, purification, and properties of recombinant barley (*Hordeum* sp.) hemoglobin. Optical spectra and reactions with gaseous ligands. *J. Biol. Chem.* **272**, 16746–16752 https://doi.org/10.1074/jbc.272.27.16746
8 Trevaskis, B., Watts, R.A., Andersson, C.R., Llewellyn, D.J., Hargrove, M.S., Olson, J.S. et al. (1997) Two hemoglobin genes in *Arabidopsis thaliana*: the evolutionary origins of leghemoglobins. *Proc. Natl Acad. Sci. U.S.A.* **94**, 12230–12234 https://doi.org/10.1073/pnas.94.22.12230
9 Kundu, S., Trent, J.T. and Hargrove, M.S. (2003) Plants, humans and hemoglobins. *Trends Plant Sci.* **8**, 387–393 https://doi.org/10.1016/S1360-1385(03)00163-8
10 Perazzolli, M., Dominici, P., Romero-Puertas, M.C., Zago, E., Zeier, J., Sonoda, M. et al. (2004) *Arabidopsis* nonsymbiotic hemoglobin AHb1 modulates nitric oxide bioactivity. *Plant Cell* **16**, 2785–2794 https://doi.org/10.1105/tpc.104.025379
11 Tiso, M., Tejero, J., Kenney, C., Frizzell, S. and Gladwin, M.T. (2012) Nitrite reductase activity of nonsymbiotic hemoglobins from *Arabidopsis thaliana*. *Biochemistry* **51**, 5285–5292 https://doi.org/10.1021/bi300570v
12 Sturms, R., DiSpirito, A.A. and Hargrove, M.S. (2011) Plant and cyanobacterial hemoglobins reduce nitrite to nitric oxide under anoxic conditions. *Biochemistry* **50**, 3873–3878 https://doi.org/10.1021/bi2004312
13 Sturms, R., DiSpirito, A.A., Fulton, D.B. and Hargrove, M.S. (2011) Hydroxylamine reduction to ammonium by plant and cyanobacterial hemoglobins. *Biochemistry* **50**, 10829–10835 https://doi.org/10.1021/bi201425f
14 Smagghe, B.J., Trent, J.T. and Hargrove, M.S. (2008) NO dioxygenase activity in hemoglobins is ubiquitous in vitro, but limited by reduction in vivo. *PLoS ONE* **3**, e2039 https://doi.org/10.1371/journal.pone.0002039
15 Wang, X. and Hargrove, M.S. (2013) Nitric oxide in plants: the roles of ascorbate and hemoglobin. *PLoS ONE* **8**, e82611 https://doi.org/10.1371/journal.pone.0082611
16 Jokipii-Lukkari, S., Kastaniotis, A.J., Parkash, V., Sundstrom, R., Leiva Eriksson, N., Nymalm, Y. et al. (2016) Dual targeted poplar ferredoxin NADP(+) oxidoreductase interacts with hemoglobin 1. *Plant Sci.* **247**, 138–149 https://doi.org/10.1016/j.plantsci.2016.03.013
17 Igamberdiev, A.U., Seregelyes, C., Manac'h, N. and Hill, R.D. (2004) NADH-dependent metabolism of nitric oxide in alfalfa root cultures expressing barley hemoglobin. *Planta* **219**, 95–102 https://doi.org/10.1007/s00425-003-1192-3
18 Eriksson, L., Pin, N., Kraft, P., Dohm, T., Minoche, J.C., Himmelbauer, A.E. et al. (2014) Differential expression patterns of non-symbiotic hemoglobins in sugar beet (*Beta vulgaris* ssp. *vulgaris*). *Plant Cell Physiol.* **55**, 834–844 https://doi.org/10.1093/pcp/pcu027
19 Panella, L. (2010) Sugar beet as an energy crop. *Sugar Tech.* **12**, 288–293 https://doi.org/10.1007/s12355-010-0041-5
20 Gordillo-Bastidas, E., Díaz-Rizzolo, D.A., Roura, E., Massanés, T. and Gomis, R. (2016) Quinoa (*Chenopodium quinoa* Willd), from nutritional value to potential health benefits: an integrative review. *J. Nutr. Food Sci* **6**, 497 https://doi.org/10.4172/2155-9600.1000497
21 Dordas, C., Rivoal, J. and Hill, R.D. (2003) Plant haemoglobins, nitric oxide and hypoxic stress. *Ann. Bot.* **91**, 173–178 https://doi.org/10.1093/aob/mcf115
22 Hill, R.D. (2012) Non-symbiotic haemoglobins-What's happening beyond nitric oxide scavenging? *AoB Plants* **2012**, pls004 https://doi.org/10.1093/aobpla/pls004
23 Sinclair, P.R., Gorman, N. and Jacobs, J.M. (2001) Measurement of heme concentration. *Curr. Prot. Toxicol.* Chapter 8, Unit 8.3 https://doi.org/10.1002/0471140856.tx0803s00

24 Onnerfjord, P., Ekstrom, S., Bergquist, J., Nilsson, J., Laurell, T. and Marko-Varga, G. (1999) Homogeneous sample preparation for automated high throughput analysis with matrix-assisted laser desorption/ionisation time-of-flight mass spectrometry. *Rapid Commun. Mass Spectrom.* **13**, 315–322 https://doi.org/10.1002/(SICI)1097-0231(19990315)13:5<315::AID-RCM483>3.0.CO;2-C
25 Huang, Z., Shiva, S., Kim-Shapiro, D.B., Patel, R.P., Ringwood, L.A., Irby, C.E. et al. (2005) Enzymatic function of hemoglobin as a nitrite reductase that produces NO under allosteric control. *J. Clin. Invest.* **115**, 2099–2107 https://doi.org/10.1172/JCI24650
26 Hargrove, M.S., Brucker, E.A., Stec, B., Sarath, G., Arredondo-Peter, R., Klucas, R.V. et al. (2000) Crystal structure of a nonsymbiotic plant hemoglobin. *Structure* **8**, 1005–1014 https://doi.org/10.1016/S0969-2126(00)00194-5
27 Mukhi, N., Dhindwal, S., Uppal, S., Kumar, P., Kaur, J. and Kundu, S. (2013) X-ray crystallographic structural characteristics of *Arabidopsis* hemoglobin I and their functional implications. *Biochim. Biophys. Acta* **1834**, 1944–1956 https://doi.org/10.1016/j.bbapap.2013.02.024
28 Smagghe, B.J., Sarath, G., Ross, E., Hilbert, J.L. and Hargrove, M.S. (2006) Slow ligand binding kinetics dominate ferrous hexacoordinate hemoglobin reactivities and reveal differences between plants and other species. *Biochemistry* **45**, 561–570 https://doi.org/10.1021/bi051902l
29 Hargrove, M.S. (2000) A flash photolysis method to characterize hexacoordinate hemoglobin kinetics. *Biophys J.* **79**, 2733–2738 https://doi.org/10.1016/S0006-3495(00)76512-X
30 Trent, J.T., Hvitved, A.N. and Hargrove, M.S. (2001) A model for ligand binding to hexacoordinate hemoglobins. *Biochemistry* **40**, 6155–6163 https://doi.org/10.1021/bi0100790
31 Doyle, M.P., Pickering, R.A., DeWeert, T.M., Hoekstra, J.W. and Pater, D. (1981) Kinetics and mechanism of the oxidation of human deoxyhemoglobin by nitrites. *J. Biol. Chem.* **256**, 12393–12398
32 Kumar, N., Astegno, A., Chen, J., Giorgetti, A. and Dominici, P. (2016) Residues in the distal heme pocket of *Arabidopsis* non-symbiotic hemoglobins: implication for nitrite reductase activity. *Int. J. Mol. Sci.* **17**, E640 https://doi.org/10.3390/ijms17050640
33 Tiso, M., Tejero, J., Basu, S., Azarov, I., Wang, X., Simplaceanu, V. et al. (2011) Human neuroglobin functions as a redox-regulated nitrite reductase. *J. Biol. Chem.* **286**, 18277–18289 https://doi.org/10.1074/jbc.M110.159541
34 Mack, G. and Tischner, R. (1990) The effect of endogenous and externally supplied nitrate on nitrate uptake and reduction in sugarbeet seedlings. *Planta* **182**, 169–173 https://doi.org/10.1007/BF00197106
35 Gniazdowska, A., Babańczyk, T. and Khasuska, U. (2012) Nitric oxide as germination controlling factor in seeds of various plant species. *Phyton - Annales Rei Botanicae* **52**, 219–226 https://academicpublishingplatforms.com/journal.php?journal=PARB
36 Catusse, J., Strub, J.M., Job, C., Van Dorsselaer, A. and Job, D. (2008) Proteome-wide characterization of sugarbeet seed vigor and its tissue specific expression. *Proc. Natl Acad. Sci. U.S.A.* **105**, 10262–10267 https://doi.org/10.1073/pnas.0800585105
37 Misra, A.N., Vladkova, R., Singh, R., Misra, M., Dobrikova, A.G. and Apostolova, E.L. (2014) Action and target sites of nitric oxide in chloroplasts. *Nitric Oxide* **39**, 35–45 https://doi.org/10.1016/j.niox.2014.04.003
38 Jasid, S., Simontacchi, M., Bartoli, C.G. and Puntarulo, S. (2006) Chloroplasts as a nitric oxide cellular source. Effect of reactive nitrogen species on chloroplastic lipids and proteins. *Plant Physiol.* **142**, 1246–1255 https://doi.org/10.1104/pp.106.086918
39 Beligni, M.V. and Lamattina, L. (2000) Nitric oxide stimulates seed germination and de-etiolation, and inhibits hypocotyl elongation, three light-inducible responses in plants. *Planta* **210**, 215–221 https://doi.org/10.1007/PL00008128
40 Coumans, M., Côme, D. and Gaspar, T. (1976) Stabilized dormancy in sugarbeet fruits. I. Seed coats as a physicochemical barrier to oxygen. *Botanical Gazette* **137**, 274–278 https://doi.org/10.1086/336870
41 Richard, G., Raymond, P., Corbineau, F. and Pradet, A. (1989) Effect of the pericarp on sugar-beet (*Beta-Vulgaris* L) seed-germination - study of the energy-metabolism. *Seed Sci. Technol.* **17**, 485–497 https://www.seedtest.org/en/content—1–1084.html
42 Hermann, K., Meinhard, J., Dobrev, P., Linkies, A., Pesek, B., Hess, B. et al. (2007) 1-Aminocyclopropane-1-carboxylic acid and abscisic acid during the germination of sugar beet (Beta vulgaris L.): a comparative study of fruits and seeds. *J. Exp. Bot.* **58**, 3047–3060 https://doi.org/10.1093/jxb/erm162
43 Chen, F., Hao, Y., Yin, Z., Wu, G. and Jiang, X. (2017) Transcriptome of wax apple (*Syzygium samarangense*) provides insights into nitric oxide-induced delays of postharvest cottony softening. *Acta Physiol. Plant.* **39**, 273 https://doi.org/10.1007/s11738-017-2569-4
44 Borisjuk, L., Macherel, D., Benamar, A., Wobus, U. and Rolletschek, H. (2007) Low oxygen sensing and balancing in plant seeds: a role for nitric oxide. *New phytol.* **176**, 813–823 https://doi.org/10.1111/j.1469-8137.2007.02226.x
45 Ioanitescu, A.I., Dewilde, S., Kiger, L., Marden, M.C., Moens, L. and Van Doorslaer, S. (2005) Characterization of nonsymbiotic tomato hemoglobin. *Biophys. J.* **89**, 2628–2639 https://doi.org/10.1529/biophysj.105.060582
46 Sainz, M., Perez-Rontome, C., Ramos, J., Mulet, J.M., James, E.K., Bhattacharjee, U. et al. (2013) Plant hemoglobins may be maintained in functional form by reduced flavins in the nuclei, and confer differential tolerance to nitro-oxidative stress. *Plant J.* **76**, 875–887 https://doi.org/10.1111/tpj.12340
47 Calvo-Begueria, L., Cuypers, B., Van Doorslaer, S., Abbruzzetti, S., Bruno, S., Berghmans, H. et al. (2017) Characterization of the heme pocket structure and ligand binding kinetics of non-symbiotic hemoglobins from the model legume *Lotus japonicus*. *Front. plant sci.* **8**, 407 https://doi.org/10.3389/fpls.2017.00407
48 Hoy, J.A., Robinson, H., Trent, J.T., Kakar, S., Smagghe, B.J. and Hargrove, M.S. (2007) Plant hemoglobins: a molecular fossil record for the evolution of oxygen transport. *J. Mol. Biol.* **371**, 168–179 https://doi.org/10.1016/j.jmb.2007.05.029
49 Smagghe, B.J., Kundu, S., Hoy, J.A., Halder, P., Weiland, T.R., Savage, A. et al. (2006) Role of phenylalanine B10 in plant nonsymbiotic hemoglobins. *Biochemistry* **45**, 9735–9745 https://doi.org/10.1021/bi060716s
50 Bruno, S., Faggiano, S., Spyrakis, F., Mozzarelli, A., Abbruzzetti, S., Grandi, E. et al. (2007) The reactivity with CO of AHb1 and AHb2 from *Arabidopsis thaliana* is controlled by the distal HisE7 and internal hydrophobic cavities. *J. Am. Chem. Soc.* **129**, 2880–2889 https://doi.org/10.1021/ja066638d